Computational Fluid Dynamics-Based Study of an Oilfield Separator—Part I: A Realistic Simulation

Ali Pourahmadi Laleh and **William Y. Svrcek,** University of Calgary, and **Wayne D. Monnery,** Chem-Pet Process Tech Limited

Summary

A realistic computational fluid dynamics (CFD) simulation of a field three-phase separator has been developed. This realistic CFD simulation provides an understanding of both the microscopic and macroscopic features of the three-phase separation phenomenon. For simulation purposes, an efficient combination of two multiphase models of the commercial CFD software, Fluent 6.3.26 (ANSYS 2006a), was implemented. The flow-distributing baffles and wire mesh demister were also modeled using the porous media model. Furthermore, a useful approach to estimating the particle size distribution in oilfield separators was developed. The simulated fluid-flow profiles are realistic and the predicted separation efficiencies are consistent with oilfield experience.

Introduction

Once a crude oil has reached the surface, it must be processed so that it can be sent either to storage or to a refinery for further processing. In fact, the main purpose of the surface facilities is to separate the produced multiphase stream into its vapor and liquid fractions. On production platforms, a multiphase separator is usually the first equipment through which the well fluid flows, followed by other equipment such as heaters, exchangers, and distillation columns. Consequently, a properly sized primary multiphase separator can increase the capacity of the entire facility.

CFD simulation is routinely used to modify the design and to improve the operation of most types of chemical process equipment, combustion systems, flow measurement and control systems, material handling equipment, and pollution control systems (Shelley 2007). There are two approaches to developing CFD models of a multiphase flow: the Euler-Lagrange approach and the Euler-Euler approach. In the Euler-Lagrange approach, the continuous fluid phase is modeled by solving the time-averaged Navier-Stokes equations, and the dispersed phase is simulated by tracking a large number of droplets through the flow field based on Newton's second law. The Euler-Euler approach, on the other hand, deals with the multiple phases as continuous phases that interact with each other. Because the volume of a phase cannot be occupied by the other phases, phase-volume fractions are assumed to be continuous functions of space and time, and their sum is equal to 1.

The literature on the critical unit operation of multiphase separators abounds with macro studies and design methodologies for two- and three-phase vertical and horizontal separators. However, there are very few papers that focus on the micro details of the actual separation process. The most important features of these studies have been reviewed as follows. Hansen et al. (1993) presented the simulation results of the developed CFD code, FLOSS, for an industrial scale three-phase separator. The separator of interest, with diameter of 3.33 m and length of 16.30 m, was the first stage of the three-stage-dual-train production process installed on Gullfaks-A offshore platform. The production on the Gullfaks-A platform started successfully in 1986–87. However, because of a projected increase in the water production, several separation inefficiencies such as water-level control, emulsion problems, and increased impurities were experienced in the following years. In order to develop an in-depth understanding of this complex three-phase separation process, Hansen et al. (1993) developed a CFD model of the separator. Because of the problem scale and importance, and also because almost all of the operating and physical parameters required for CFD simulations have been provided by Hansen et al. (1993), this significant case was selected for comprehensive CFD studies in the present work. Hallanger et al. (1996) developed a CFD model for a three-phase (free gas, oil+dispersed water, and free water) separator by extension of the two-fluid model. The mixture model was used for modeling the oil phase while the water droplets were distributed through different droplet size classes. The momentum equation for the mixture phase together with the continuity equations for each class was solved. Interaction between dispersed droplets, such as coalescence and breakup, was neglected. The pressure-correction approach with some adjustments for the mixture phase was used to obtain the numerical solution of the system. The model was used to simulate a first-stage separator equipped with a deflector baffle, two perforated baffles, a demister, and a weir plate. The CFD results indicated that most of the smaller water droplets would remain in the oil phase. The CFD results in terms of concentrations of water droplets in the oil outlet vs. oil-residence time compared well with empirical data. The effects of inlet distributors and distributing baffles on reducing the size and weight of separation trains were reviewed by Frankiewicz et al. (2001). The sensitivity of the installed vortex cluster to the inlet flow rate has also been demonstrated. This paper did not include any information on the developed CFD models. Frankiewicz and Lee (2002) studied the influence of inlet nozzle configuration, flow distributors, perforated plates, and outlet nozzles on the flow pattern in two and three-phase oilfield separators. They used Fluent 6.0 software and took the inlet nozzle, the inlet momentum breaker, perforated plates, weir or bucket plates, and outlet nozzles as the key affecting components. To increase the effective liquid retention time, CFD studies indicated that a second perforated plate just upstream of the outlet nozzle was required. Moreover, the use of composite plate electrodes and the shrouded pipe distributors increased the capacity of the operating separator to some 67% owing to an improved plug-flow regime. Lee et al. (2004) evaluated the design of internals for a three-phase separator to mitigate sloshing of liquid phases caused by the offshore platform location. In order to prevent the water phase from being pulled up toward the oil weir, on the basis of the performed CFD simulations, a perforated baffle was designed and placed near the oil weir, the open areas of two preceding baffles were decreased, and the configuration of the oil weir was modified.

Original SPE manuscript received for review 29 November 2010. Revised manuscript received for review 10 February 2011. Paper (SPE 161212) peer approved 22 March 2011.

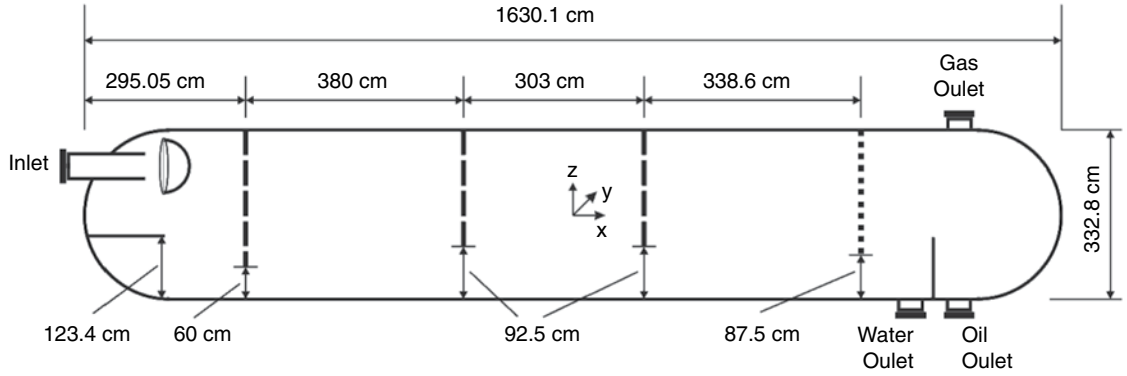

Fig. 1—Geometrical specifications of the Gullfaks-A separator (Hansen et al. 1993).

TABLE 1—QUALITY OF THE MESH PRODUCED FOR THE GULLFAKS-A SEPARATOR IN THE GAMBIT ENVIRONMENT

Number of Cells	Maximum Squish	Maximum Skewness	Maximum Aspect Ratio	
884847	0.748182	0.895873	44.1708	
Skewness of the Produced Mesh				
Skewness range	0–0.20	0.20–0.40	0.40–0.60	0.60–0.80	0.80–1.0
Density of cells	79.0416%	15.4785%	3.8489%	1.6285%	0.0025%

These improvements led to eliminating the water spillover problem. Unfortunately, the details of the CFD simulations and the obtained solutions were not presented in the paper.

A vertical two-phase separator equipped with a deflector baffle and a vane-type demister was modeled by Swartzendruber et al. (2005) using Fluent software. They focused on the quality of gas flow distribution through the demister. Again, unfortunately, details of the developed CFD model are missing from the paper. On the basis of the resulting fluid-flow streamlines, two changes were devised to mitigate the uneven flow distribution in the vane demister. Thus, the deflector baffle was moved away from the inlet and installed parallel to vane demister, and a 90° elbow with turning vanes was installed between the inlet and the deflector baffle. Lu et al. (2007) studied the effectiveness of perforated plate baffles for improving the separation performance of a FWKO separator. The Fluent 6.2 software was used for simulation, but the multiphase modeling was based only on a balance between available computational resources and model capabilities. The velocity contours of fluid flows visually confirmed that the previous large flow circulations were broken into small ones by installing the perforated plate baffles. Furthermore, the mean residence time of fluid particles was calculated and showed an increase from 630 to 980 seconds for the water phase and from 520 to 745 seconds for the oil phase because of the installed distributing baffles. Lee et al. (2009) discussed several engineering judgments and the corresponding CFD verifications to revamp the phase-separation inefficiencies experienced in a major oil production facility. Their debottlenecking studies led to some suggestions for the weir height, liquid levels, and configuration and position of distribution baffles. Again, details of the CFD models, developed through the Fluent 6.3.26 software, have not been provided in the paper. The simulation results showed that the applied improvements mainly influenced the water phase, and the fluid-flow streamlines visually confirmed that the large flow circulations were broken into small weak ones by implementing the suggested modifications.

Developed CFD Model

Physical Model. Fig. 1 provides the geometrical specifications of the Gullfaks-A separator as provided by Hansen et al. (1993). As Fig. 1 shows, a spherical deflector baffle was used to break the momentum of the inlet three-phase fluid flow entering the vessel as a high-momentum jet. The upper part of the vessel was equipped with internals, including flow-distribution baffles and a demister, to enhance the separation of liquid droplets from gas.

In this study, building the physical model and generating the corresponding mesh system were performed in the Gambit 2.4.6 (ANSYS 2006b) environment. In order to have a discretized model with "good" grid quality, the mesh-generation process was completed in a step-by-step sequence. The vessel was split into areas and the inlet nozzle, deflector baffle, splash plate, weir, and outlet nozzles were first discretized. In doing so, the edges of nozzles and other internals were discretized before the mesh generation for the separator surfaces and volumes. Then, the cylindrical part of the vessel was discretized such that some cells in this part were separated and referred to as the porous media, and did include mesh for distribution baffles and the demister pad. The horizontal surrounding surfaces of each baffle (with thickness of 0.02 m) and those of demister pad (with thickness of 0.15 m) were assumed to be flat surfaces. Therefore, in the cylindrical part of the vessel, the grids must be fine enough and arranged horizontally in regular and constant intervals. After generating the mesh for the cylindrical part of the vessel, the remaining parts of the vessel were "swept" by the Gambit mesh generation tool. Mesh elements were generally hexahedral. However, for regions with complex geometry (i.e., the inlet and outlet nozzles), tetrahedral elements were necessarily used.

The global quality of the produced mesh in terms of number of cells, maximum cell squish, maximum skewness, and maximum aspect ratio are presented in **Table 1,** and **Fig. 2** includes screen shots of the generated model in the Gambit environment. Furthermore, to ascertain the quality of the generated mesh, the cell skewness was evaluated and, as shown by the mesh results of Table 1, only a negligible fraction of cells (0.0025%) was of poor quality. However, the grids with a cell skewness factor greater than 0.8 were

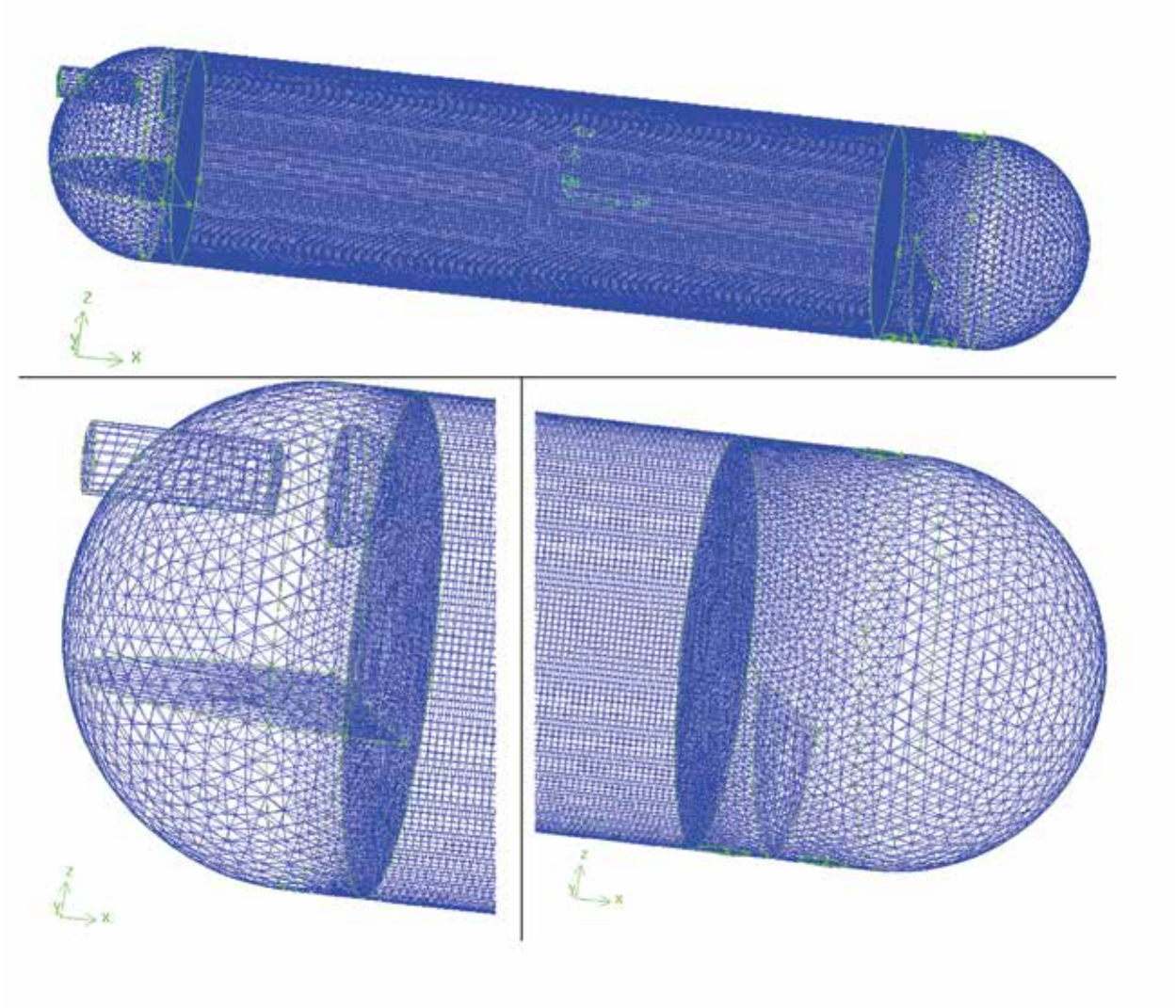

Fig. 2—Physical model and mesh generated for the Gullfaks-A separator in the Gambit environment.

TABLE 2—PHYSICAL PARAMETERS OF FLUIDS IN GULLFAKS-A SEPARATOR PROVIDED BY HANSEN ET AL. (1983)

	1988 Production Rate (m^3/h)	Future Production Rate (m^3/h)	Density (kg/m^3)	Viscosity (Pa·s)
Gas	1640	1640	49.7	1.30e–5
Oil	1840	1381	831.5	5.25e–3
Water	287	1244	1030	4.30e–4
Operating Conditions	Temperature=55.4°C; pressure=6870 kPa			

converted to polyhedral grids. Although this minor modification did not reduce the maximum values reported in Table 1, the number of cells was reduced from 884,847 to 884,805.

Material Definition. The physical parameters for the fluids in the Gullfaks-A separator are taken from Hansen et al. (1993) and presented in **Table 2.** Because interfacial surface tensions were not given in the original paper, estimated values were used. For this purpose, a hydrocarbon mixture was defined in HYSYS 3.2 (AspenTech 2003) to simulate the oil phase. The criterion for setting the composition of the mixture was the accuracy of the mixture density and viscosity at operating temperature and pressure compared to the values given in the original study. Using the PR equation of state and the TRAPP model, the density and viscosity of the mixture were estimated to be 783.59 kg/m^3, and 0.005296 Pa·s, respectively, with an estimation error for the oil density and viscosity of 5.76 and 0.88%, respectively. Thus, it was assumed that the oil/gas surface tension estimated by HYSYS was reasonable, and a surface tension of 0.0238 N/m was assumed for the oil/gas interface. The assumed value compared well with the oil surface

tension range of 0.023 to 0.038 N/m at 20°C proposed by Streeter and Wylie (1985). HYSYS 3.2 was also used for estimation of water/gas surface tension of 0.0668 N/m. Using the chart provided by Heidemann et al. (1987), the surface tension of pure water is 0.067 N/m at 55.4°C, which is in agreement with the HYSYS estimate. Finally, the empirical study of Kim and Burgess (2001) was used to estimate the oil/water surface tension of 0.052 N/m at 25°C. They noted that although oil is a mixture of various hydrocarbons, each one constituting hydrocarbon in contact with water has almost the same interfacial surface tension. Thus, it was assumed that the surface tension for oil/water interface at 25°C would be almost the same as reported by Kim and Burgess (2001). Furthermore, in order to account for surface tension temperature functionality as proposed by Poling et al. (2001), the reported value was modified and a surface tension of 0.0486 N/m was used for the oil/water interface at 55.4°C. The estimated value is in agreement with the Antonoff's rule in that the oil/water surface tension should be approximately equal to the absolute difference between oil and water surface tensions (Antonoff 1907), which are 0.0238 and 0.0668 N/m, respectively.

Modeling the Distribution Baffles. The porous media model with appropriate modifications was used to model the flow through baffles and demisters. This approach is based on the evaluation of the momentum source term in the porous media model by correlations developed by Kolodzie and Van Winkle (1957) for the fluid flow through a perforated plate (Pourahmadi Laleh 2010). Eq. 1 was developed for calculation of the inertial resistance factor C_2 in the direction normal to the baffle plate:

$$C_2 = \frac{1}{C^2\delta}\left[\left(\frac{A_p}{A_f}\right)^2 - 1\right], \quad \text{..... (1)}$$

where C is the plate discharge coefficient, δ is the baffle thickness in m, and A_p and A_f are total area and open area of the baffle in m^2, respectively. Therefore, if the configuration and dimensions of the flow-distributing baffles are provided, C_2 and the porosity of baffles, which are necessary for the porous media model, can be calculated. Although these crucial specifications were not provided in the original paper of Hansen et al. (1993), Hansen et al. (1991) performed several experiments to obtain data in order to validate the results of their developed computer code, FLOSS, which was used for the simulation of the Gullfaks-A separator. Inside their experimental model, with dimensions of 0.46×0.46×1.83 m, the flow-distributing baffle was specified as a perforated plate with 173 holes, each with diameter of 6.4 mm and distance between centers of 25 mm. Because the model has been used for validation of the computer code, and the computer code was used to simulate the Gullfaks-A separator, it can be expected that the model baffle had the same overall configuration (hole pattern) as the baffles of the Gullfaks-A separator. Therefore, with the further assumption of a baffle thickness of 20 mm, the baffle porosity ε was calculated to be 0.05, and constant C_2 was calculated to be 29240 m^{-1}.

Modeling the Wire Mesh Demister. Wire mesh demisters were also modeled using the porous media model. For this purpose, the porous media parameters, which are used for pressure drop calculations in the media, need to be set. Because the mesh pad demisters generally result in very low pressure drops, their pressure drop was assumed to be negligible. Fortunately, quite recently, a comprehensive and practical research study has appeared in the public literature that deals with the characterization of pressure drop in knitted wire mesh demisters. Helsør and Svendsen (2007) have reviewed the two other relevant studies in this field and presented their model for pressure drop calculation in mesh pads. In their experimental studies, the data have been collected and analyzed for seven different wire mesh demisters, at four different system pressures (ranging from atmospheric pressure to 9.2 MPa), using three different fluids (air, nitrogen, and natural gas). The data have been fit to a Hazen-Dupuit-Darcy type equation (Eq. 2) for calculation of the pressure drop caused by demister:

$$\frac{\Delta P}{\Delta x} = \frac{\mu}{\alpha}V + C\rho V^2, \quad \text{..... (2)}$$

where μ is the fluid viscosity in Pa·s, α is permeability factor in m^2, V is flow velocity in m/s, C is the plate discharge coefficient, and ρ is the fluid density in kg/m^3.

Helsør and Svendsen (2007) have provided the correlating parameters (α and C) for the different mesh pad types. As noted by Pourahmadi Laleh (2010), provided that the type and characteristics of the mesh pad are available, these correlating parameters can be used to calculate the parameters required for the porous media model. Because the specifications of the demister were not provided in the original paper of Hansen et al. (1993), the most commonly used wire mesh properties were assumed for calculation of these constants. A wire mesh pad with a thickness of 0.15 m is commonly used in separators (Walas 1990; Lyons and Plisga 2005; Coker 2007); hence, a type E demister as specified by Helsør and Svendsen (2007) was selected for simulation purposes. The viscous resistance factor was calculated to be 3.85e6 m^{-2}, and the inertial resistance factor was calculated to be 126 m^{-1}.

Multiphase Models Incorporated. In order to develop a visual understanding of the complex three-phase separation process, Hansen et al. (1993) modeled the overall fluid-flow regimes inside the separator. To simplify this complicated simulation task, they focused on two zones: the inlet and momentum breaker zone and the bulk liquid flow zone. In the current study, however, all the separation zones of the separator were simulated. Therefore, the results should provide an overall picture of separation quality not only in the inlet and bulk liquid zones, but also in the gas and interface zones. Exploiting the various multiphase models available in the Fluent 6.3.26 software, an efficient combination of two multiphase modeling approaches is used for modeling both the macroscopic and microscopic features of this three-phase separator. Therefore, the Euler-Lagrange approach is used for simulation of the movement of fluid droplets that are injected at the separator inlet, and the Euler-Euler approach is used for simulation of fluid-flow patterns in the immiscible three-phase flows. Implementation of the Euler-Lagrange approach leads to the discrete phase model (DPM), which works well for flow regimes in which the discrete phase is of less than 12% volume fraction. In addition to the gravity and drag forces, which are the most affecting forces in the phase-separation phenomenon, all other relatively effective forces, such as the virtual mass force, the Brownian force, and the lift force, are also taken into account while tracking the droplets in the DPM model. Coalescence of particles and their breakups are also modeled by DPM. For this purpose, the collision model is used for modeling droplet coalescence, and on the basis of the particle Weber number, a proper model within the spray model theory [i.e., the Taylor analogy breakup (TAB) model or wave model] is used for modeling droplet breakup. As the surface tracking model of the Euler-Euler approach, the volume of fluid (VOF) is used for simulation of the fluid-flow patterns. The VOF model is designed for the simulation of immiscible multiphase flows where the position of the interface between any two adjacent different phases is of interest. In this model, a single set of momentum equations is shared by the fluids, and the volume fraction of each phase in the computational cells is tracked throughout the domain. Note that the VOF is not perfect for modeling the inlet zone of a separator because a complex momentum exchange occurs in this zone and fluid phases are fully interpenetrating. However, the VOF model can effectively capture the macroscopic aspects of the major part of a multiphase separa-

TABLE 3—DISCRETE PHASE PARAMETERS USED IN CFD SIMULATION OF GULLFAKS-A SEPARATOR

	1988 Condition		Future Condition	
Discrete Phase Parameters	Oil Drops	Water Drops	Oil Drops	Water Drops
Maximum diameter (μm)	2,267	4,000	1,955	3,450
Mean diameter (μm)	907	1,600	780	1,380
Total mass flow rate (kg/s)	6.5e–4	4.4e–3	4.2e–4	2.8e–3
Number of tracked particles		1,000		
Minimum diameter (μm)		100		
Spread parameter		2.6		

tor, the gravity separation zone. The necessary model settings will be described in the following sections.

Definition of Droplet Size Distribution. In order to model the dispersion of oil and water droplets in the fluid-flow domain, the specification of the particle size distribution is a key step. However, empirical data on the size of fluid particles was not available from the Gullfaks-A separator (Hansen et al. 1993). Thus, a reliable method was required for prediction of particle size distribution for oil and water droplets entering the separator. There are numerous research studies that predict the size distribution of fluid dispersions. However, most have focused on prediction of maximum stable droplet size because the other necessary size distribution parameters such as spread parameter and minimum and mean droplet size can be estimated based on the predicted (or measured) maximum stable droplet size and the nature of the fluid phases. In the present study, the common particle size distribution function, the Rosin-Rammler (1933) equation, has been used. The Rosin-Rammler equation contains two parameters: volume mean diameter $\overline{d}$ and spread parameter n:

$$Y_d = \exp\left[-\left(\frac{d}{\overline{d}}\right)^n\right], \quad \text{..... (3)}$$

where Y_d is the mass (or volume) fraction of droplets with diameter greater than d.

In Eq. 3, the volume mean diameter $\overline{d}$ can be estimated from maximum droplet diameter, d_{max}, through Eq. 4, proposed by Green and Perry (2007):

$$\overline{d} = 0.4\, d_{max} \quad \text{..... (4)}$$

To specify the spread parameter n for the Gullfaks-A dispersions, two experimental studies, performed by Karabelas (1978) and Angeli and Hewitt (2000), were used. The experiments of Karabelas were carried out with kerosene (ρ=798 kg/m^3, μ=0.00182 Pa·s) and a more viscous transformer oil (ρ=892 kg/m^3, μ=0.0156 Pa·s) as continuous phases and water as dispersed phase. The experiments of Angeli and Hewitt were performed with both water and the oil (ρ=801 kg/m^3, μ=0.0016 Pa·s) as dispersed and/or continuous phases. The experimental distributions of Angeli and Hewitt produced a value between 2.1 and 2.8 for the Rosin-Rammler spread parameter. This result agrees with the values of 2.13 to 3.30 reported by Karabelas (1978) for water dispersed in two different oils. One of the most interesting experimental results of the Karabelas (1978) study showed that the spread parameter can be assumed to be constant and close to the measured average value for either oil in water or water in oil dispersions. Therefore, the arithmetic average value of 2.6, as reported by Karabelas (1978), was used to set the particle size distribution.

The next step involved finding a reliable method for prediction of maximum stable oil and water droplet sizes. The fundamental study in the field of droplet dispersions in the turbulent flow was conducted independently by Kolmogorov (1949) and Hinze (1955). They assumed that the maximum stable droplet or bubble size d_{max} could be determined by the balance between the turbulent pressure fluctuations, tending to deform or break the droplet or bubble, and the surface tension force resisting any deformation. The other important theory for maximum stable bubble size was developed later by Levich (1962). He assumed that the maximum stable droplet or bubble size d_{max} could be determined by the balance between the internal pressure of the droplet or bubble and the capillary pressure of the deformed droplet or bubble. In a later study, Hesketh et al. (1987) modified the Levich theory to develop an equation that includes all the salient physical fluid properties required to describe droplet or bubble size in turbulent flow. Hesketh et al. (1987) considered both the Kolmogorov-Hinze and Levich theories and recognized that in predicting maximum particle size for liquid/liquid and gas/liquid dispersions, only the latter gives consistent results. By including a viscosity grouping term originally proposed by Hinze (1955), Hesketh et al. (1987) have developed the following generalized equation:

$$d_{max} = 1.38\left(\frac{\sigma^{0.6}}{\rho_c^{0.3}\rho_t^{0.2}\mu_{dc}^{0.1}}\right)\left(\frac{D^{0.5}}{V_c^{1.1}}\right) \times\left(1+0.5975\left[\frac{\mu_d\left(\mu_c^{0.25}V_c^{2.75}\rho_c^{-0.25}D^{-1.25}d_{max}\right)^{1/3}}{\sigma}\right]\sqrt{\frac{\rho_c}{\rho_d}}\right)^{0.6} \quad \text{..... (5)}$$

where ρ_c and ρ_d are the continuous and dispersed phase densities (respectively) in kg/m^3, μ_c and μ_d are the continuous and dispersed phase viscosities (respectively) in Pa·s, D is inside diameter of pipe in m, and V_c is superficial velocity of continuous phase in m/s. Note that d_{max} should be calculated from Eq. 5 in an iterative manner, because d_{max} is also present on the right side of Eq. 5 with an exponent of 0.2.

Although estimation of d_{max} using Eq. 5 is tedious, the strong theoretical background and its very satisfactory representation of empirical data provided confidence in using this method for prediction of the maximum droplet size. Note that Hesketh et al. (1987) showed that this approach provided excellent results when dealing with experimental data that included a broad range of physical properties: surface tension of 0.005 to 0.072 N/m, the continuous phase viscosity of 0.001 to 0.016 Pa.s, and the dispersed phase density of 1 to 1000 kg/m^3.

The discrete phase parameters required for CFD simulation of the Gullfaks-A separator have been calculated and presented in **Table 3.** The droplet size distributions for oil and water dispersions are also represented in **Fig. 3.**

Setting the CFD Simulator Parameters. The Reynolds number was much more than the transient value (Re=2,300) for all fluid phases, and a suitable turbulence model was selected as the viscous

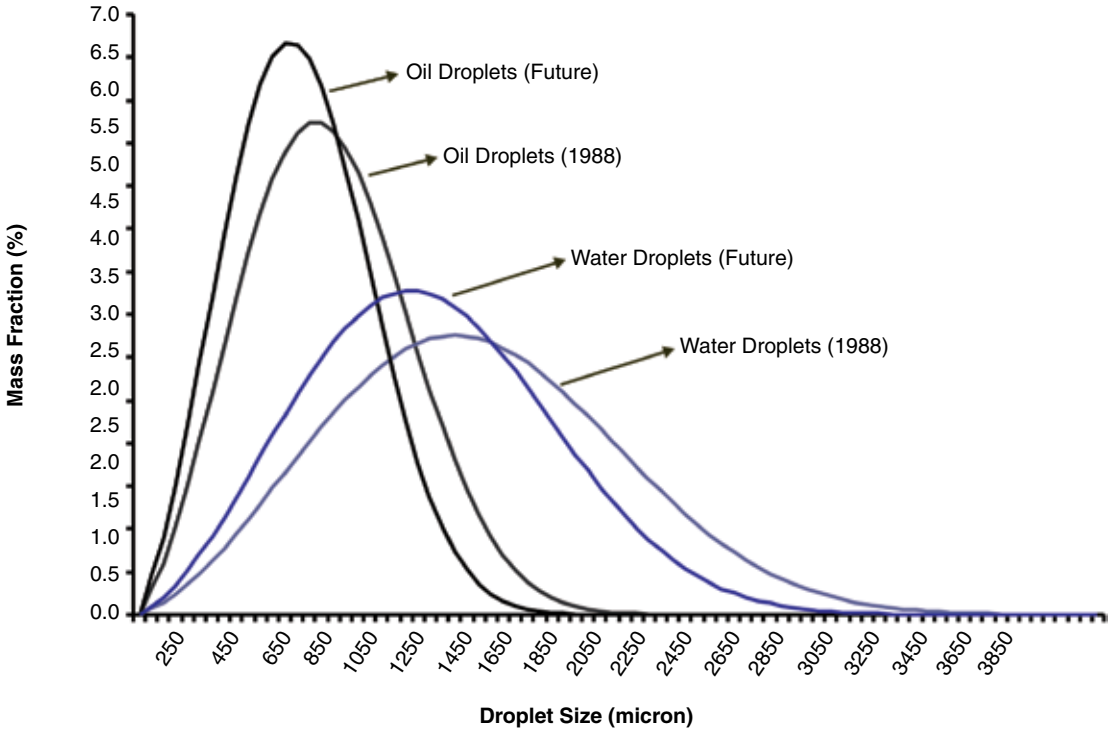

Fig. 3—Droplet size distributions for oil and water dispersions at 1988 and the future production conditions.

model. For this purpose, the standard $k-\varepsilon$ (Launder and Spalding 1972) model was selected. This semi-empirical model has been selected as the default in most commercial packages and is accepted as the most cost-effective and widely applicable turbulence model (Sharratt 1990; Gosman 1998).

In order to input the boundary conditions for inlet, the velocity and volume fractions of phases were set. For the gas-outlet boundary, outlet pressure and volume fractions (as pure gas) were set while for the liquid-outlet boundaries, outlet velocities and volume fractions (as pure liquid) were set. For identifying the flow regimes in inlet and outlet nozzles, the turbulence intensity and hydraulic diameter of flow through the nozzles were determined. The turbulence intensity in the inlet and outlet zones was estimated using an empirical correlation (Fluent 6.3 User's Guide 2006):

$$I=0.16\,\mathrm{Re}^{-0.125} \quad \ldots\ldots (6)$$

In normal operation, the separator was half-filled with liquid (Hansen et al. 1993). To set the position of interface between phases, the volume fractions of phases above and below the assumed interface were patched to the reasonable values.

Solving a multiphase simulation problem is inherently subject to stability and convergence issues. Careful choice of the solution method and under-relaxation factors markedly affects both the rate of convergence and the solution existence (Sharratt 1990; Anderson 1995). Thus, in order to overcome the stability/convergence difficulties, the pressure-implicit with splitting of operators (PISO) method was used as the solver (Issa 1986), and the under-relaxation factor for pressure, density, momentum, volume fraction, and turbulence groups was set at 0.10, 0.90, 0.0005, 0.005, and 0.70, respectively.

Results and Discussion

Before presenting the results of this case study, it is important to highlight the most important modifications of this study as compared with the original research presented by Hansen et al. (1993). In their CFD simulation of this multiphase separator, Hansen et al. (1993) made a number of simplifying assumptions:

- Fluid-flow analysis was confined to the inlet zone and the bulk liquid flow zone. Therefore, the interaction between multiple zones was ignored.
- In both zones, the flow was considered to be symmetrical around the vertical plane in the middle of the separator (xz-plane); thus, only half of each zone volume was modeled. Apparently, this is a questionable assumption, particularly when no plug flow regime was established as shown by their results.
- The inlet section of the separator in which all three phases are present was modeled as a two-phase gas/liquid flow, and the results did provide the boundary conditions for the distributed velocity field in the liquid pool. A two-phase simulation of a three-phase zone will reduce the accuracy of the results for the inlet zone, and the incorrect boundary condition will also decrease the accuracy of downstream bulk liquid solution flow.
- The grid systems used for numerical simulations of the inlet zone and the bulk liquid zone were $11\times8\times15$ and $23\times4\times5$, respectively. Given the vessel dimensions, the generated grid systems are rather coarse. Note that if the assumed grid system was developed such as to cover whole the vessel, the generated grid would include some 4,480 cells, which is 0.51% of the generated mesh cells of the developed CFD model. Therefore, the grid system of the current study is almost 200 times finer than that used in the original work of Hansen et al. (1993).
- The other major improvement when compared with not only Hansen et al. (1993) but also other previous projects on the CFD-based study of separator performance is the direct and quantitative evaluation of the separator efficiency. For this purpose, five data-recording planes were defined to record the characteristics of the droplets passing through them. The recording surfaces of interest were two vertical at the start and at the end of the gravity separation section, the gas outlet, the oil outlet, and the water outlet. Computer codes were developed to analyze the data provided by the recording planes. These computer codes calculate the separation efficiencies (based on mass distribution of droplets among gas, oil, and water outlets), Rosin-Rammler particle size distributions on the five capturing surfaces, and the number of droplet coalescence and breakup.

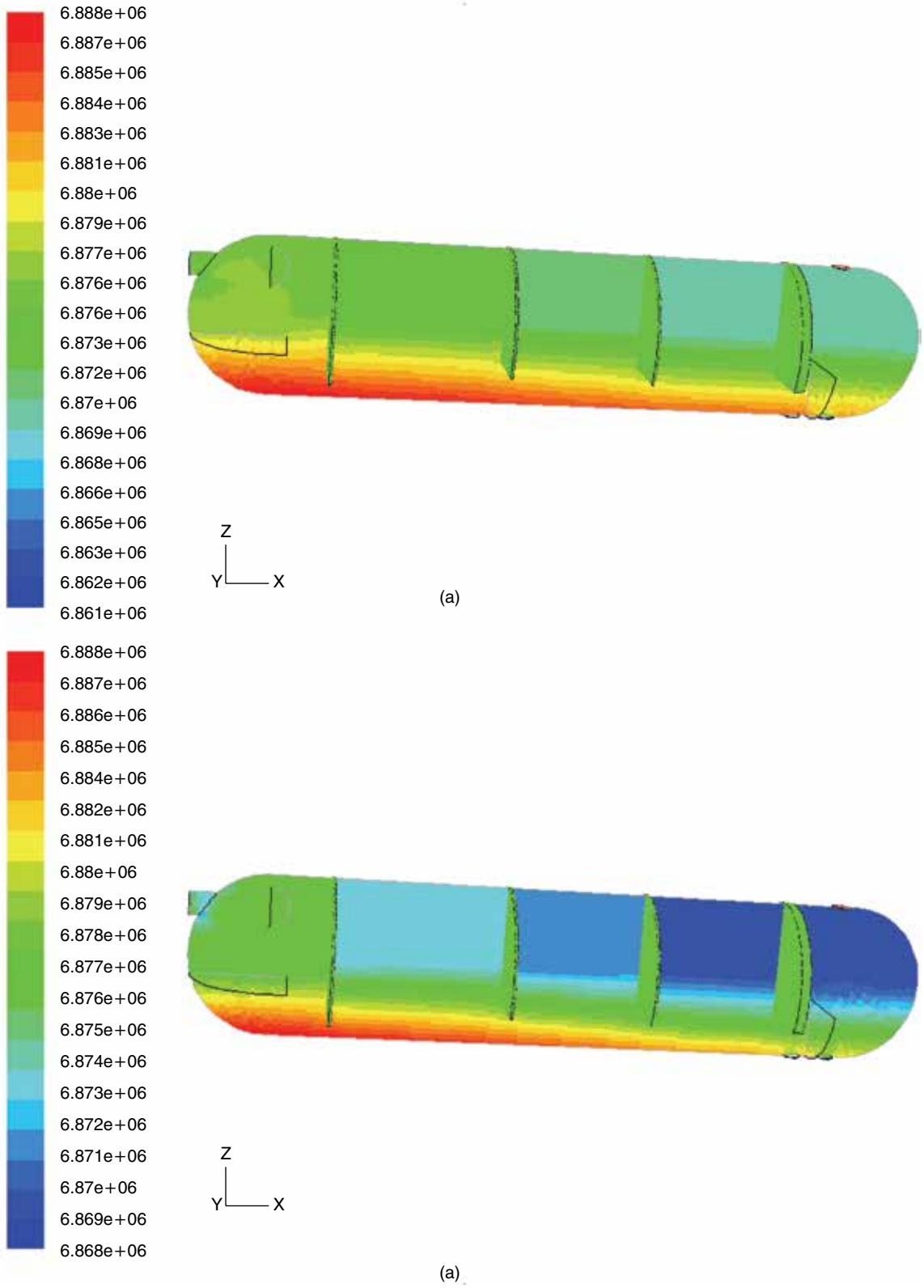

Fig. 4—Contours of pressure (Pa) in the middle of the Gullfaks-A separator for (a) 1988 and (b) the future condition.

Having prepared the physical model and set all the CFD parameters, some 4,000 iterations were required for the continuous-phase solution convergence. Each iteration took approximately 22 seconds on a Pentium D (3.20 GHz) and 2.00 GB of RAM PC. Therefore, a PC runtime of approximately 24 hours was required for solution of continuous-phase fluid flows with a further PC runtime of approximately 3 hours required for the simulation of interactions among the dispersed droplets and the continuous phases.

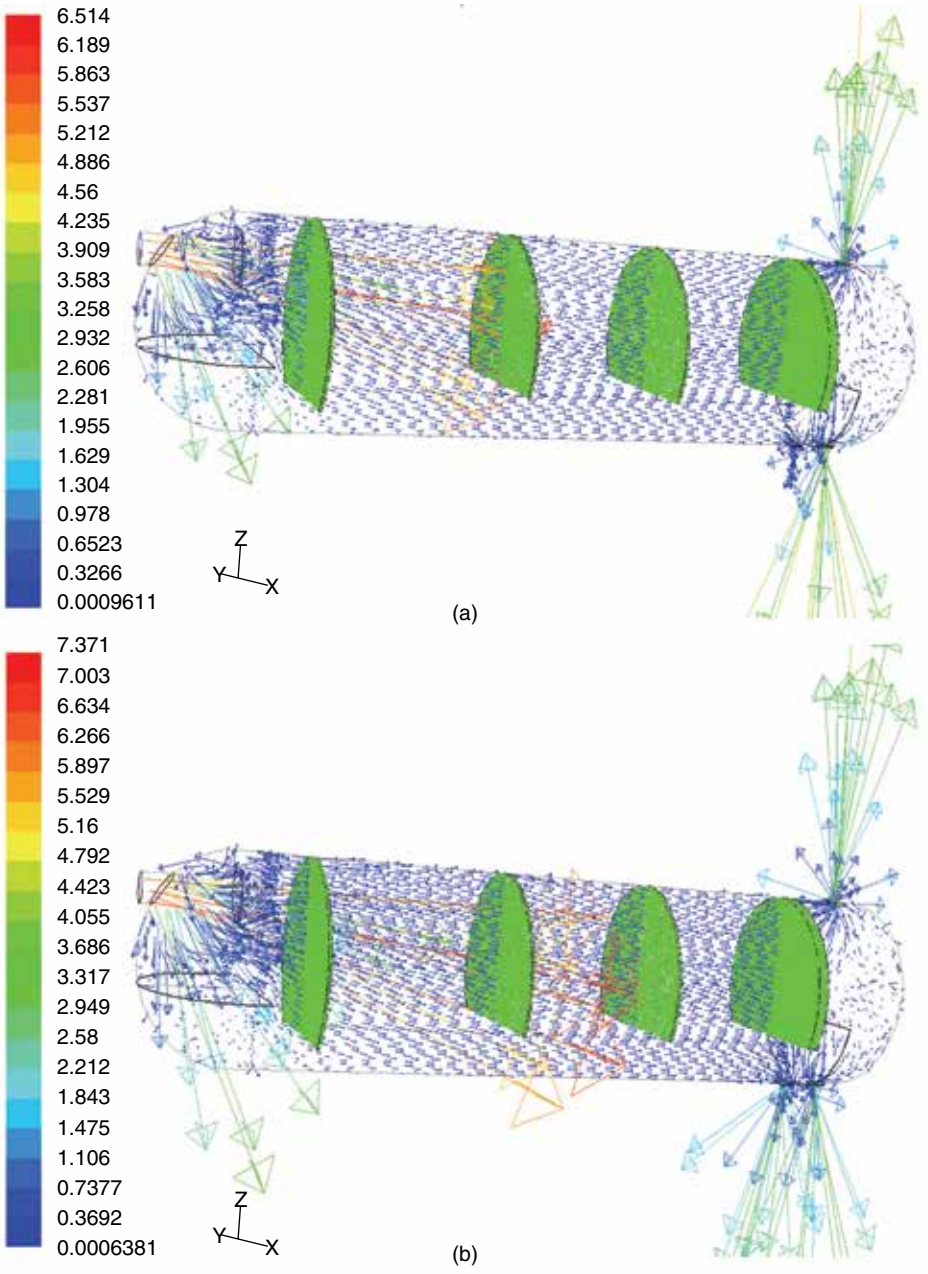

Fig. 5—Vectors of velocity (m/s) in the middle of the Gullfaks-A separator for (a) 1988 and (b) the future condition.

Fluid-Flow Profiles. Velocity vectors on four parallel horizontal planes and four parallel vertical planes for both the 1988 and the future production condition were obtained and compared with the corresponding profiles from the original study. A complete set of the profiles has been provided in Pourahmadi Laleh (2010), but the most significant profiles will be presented in this paper. Using the original profiles, Hansen et al. (1993) addressed the rotational flow regimes established between any two internals. However, the large-scale fluid-flow circulations were not realized in current study, even though some minor flow circulations or backflows were predicted. It was noted during the solution convergence trend that if the over-relaxation parameters are not adjusted correctly or the correct solver is not selected, large rotational flow patterns can be produced, and the solution fluctuates without approaching a realistic converged solution. In addition to this issue, the major simplifying assumptions used in the original work are another probable source of inaccuracy. Therefore, it would seem that the large flow circulations predicted by Hansen et al. (1993) are a result of poor adjustments or assumptions (e.g., the poor setting of the over-relaxation parameters). Furthermore, the recent CFD-based study by Lu et al. (2007) does show that the distribution baffles generally improve the quality of liquid flow distribution in the vessel, break the large-scale circulations into smaller ones, and reduce the short-circuiting flow streams.

The pressure, velocity, and density profiles for both production conditions are shown in **Figs. 4 through 6.** The simulated pressure profiles indicated that the pressure drops assigned to the baffles and demister are small (reasonable), and the velocity vectors were realistic. However, on the basis of the simulated density contours (Fig. 6), it would seem that the separator at both operating conditions (particularly, at the future production condition) may suffer from foam and emulsion problems. The distortion of interfaces in the inlet and outlet zones indicates a potential for foam and emulsion problems. The other detectable problem is the flow behavior near

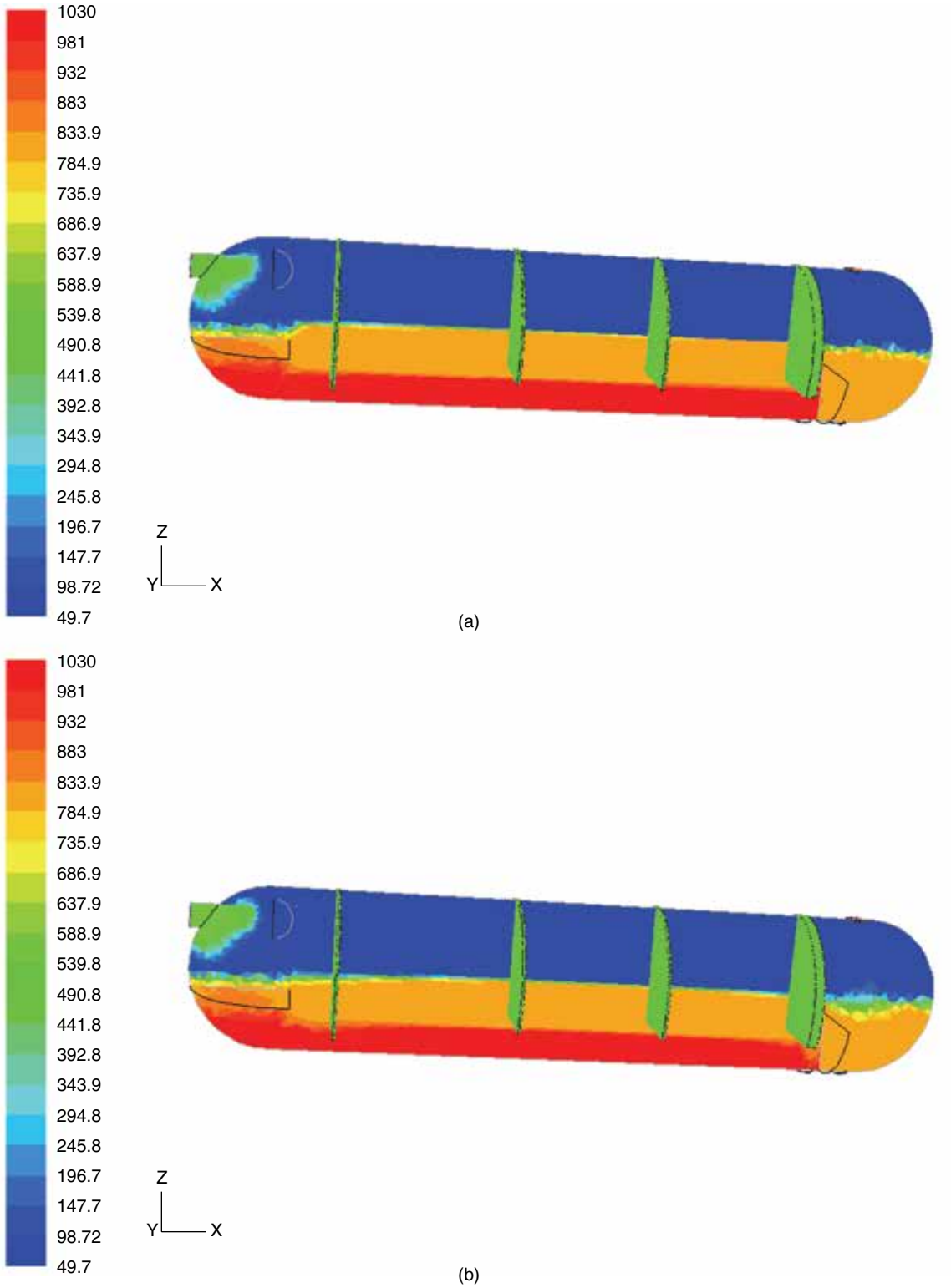

Fig. 6—Contours of density (kg/m^3) in the middle of the Gullfaks-A separator for (a) 1988 and (b) the future condition.

the water outlet predicted for the future production condition (Fig. 6b). With the large increase in the produced water flow rate, the water phase must be pumped from the vessel at much higher rates. Therefore, as indicated by the present CFD simulation results, there is an increasing tendency for the oil phase to be pushed toward the water outlet. This, at least, will increase the risk of turbulence in the water outlet zone and may lead to mixing of the phases. In order to overcome this problem, one should minimize the risk of mixing liquid phases by improving the vessel design.

Separation Efficiencies. The analysis of the oil and water droplets exiting at the separator outlets resulted in a predicted overall separation efficiency of 98.0% at the 1988 production conditions. The result is based on the mass distribution of injected oil and water

TABLE 4—DROPLET SIZE DISTRIBUTION IN IMPORTANT ZONES OF THE GULLFAKS-A SEPARATOR

		Discrete Phase Parameters	Before Gravity Separation Zone	After Gravity Separation Zone	Oil Outlet	Water Outlet
1988 Production Condition	Oil Droplets	d_{min} (μm)	26	26	26	–
		d_{max} (μm)	1848	1830.3	1209	–
		$\bar{d}$ (μm)	640	627	419	–
		n	3.18	3.20	3.80	–
	Water Droplets	d_{min} (μm)	85	85	93	90
		d_{max} (μm)	2423	2338	438	2315
		$\bar{d}$ (μm)	1077	1009	257	1008
		n	2.81	2.79	6.79	3.05
Future Production Condition	Oil Droplets	d_{min} (μm)	37	37	47	25
		d_{max} (μm)	1009	1009	219	855
		$\bar{d}$ (μm)	422	423	154	300
		n	4.42	4.43	6.55	3.60
	Water Droplets	d_{min} (μm)	34	34	76	34
		d_{max} (μm)	1596	1596	148	1593
		$\bar{d}$ (μm)	643	633	132	545
		n	4.11	3.55	6.60	3.67

droplets at the separator outlets. This mass distribution analysis indicated that 100% of oil droplets and 96.9% of water droplets were separated and exited through their corresponding outlets. Note that there was no droplet present in the gas phase outlet; hence, all the injected droplets came out in either the oil outlet or the water outlet.

As would be expected from practical field experience and also shown in the density contours of Fig. 6b, with an increase at the future produced water flow rate, the separation efficiency for oil droplets was predicted to decrease to 1.3%. Again, there was no predicted carryover in the gas outlet, and thus all the injected droplets came out with either the oil outlet or the water outlet. Therefore, the gas/liquid separation efficiency was still 100%. The very low separation efficiency for oil droplets indicates that the water phase does not have sufficient residence time for oil droplets to rise up and join the oil phase; therefore, almost all of the oil droplets are carried by water phase to the water outlet. Although the separation efficiency was calculated to be 100% for water droplets, because of the difficulty in separating the oil droplets, the total separation efficiency has been reduced to 70.4%.

The result of droplet size distribution analysis on the selected surfaces of the separator is shown in **Table 4.** As the data of Table 4 shows, when compared with the initially defined droplet size distribution (Table 3), droplets have become smaller. The reason is that droplet breakup occurs when the injected droplets strike the deflector baffle. Therefore, the volume median diameter has decreased to 70% of its initial value for oil droplets, and to 67% of its initial value for water droplets for the 1988 production condition. With the projected increase in the inlet water flow rate, these values change to 54% for oil droplets and to 46% for water droplets. The CFD simulation results show that for the 2,000 injected droplets, the number of breakups was predicted to be 1,590 for 1988 condition and 1,543 at the future operating condition. Free coalescence of droplets was not a common phenomenon in the three-phase separator. Droplet coalescence may happen at a very low rate of approximately 0.1% without any noticeable trend. Table 4 also shows that the droplet size distribution before and after the gravity separation zone is almost the same. This implies that there should be no further breakup while droplets are traveling through the main part of the separator; hence, droplet size distribution remains essentially constant.

Conclusions

A three-phase separator located in the Gullfaks oilfield in the Norwegian sector of the North Sea was simulated. The combined VOF-DPM approach was used to capture both macroscopic and microscopic features of the phase-separation phenomenon. In this study, the installed distribution baffles and mist eliminator were modeled using the porous media model, which required the detailed specifications and design information for the three-phase separator. Using the available theoretical approaches and experimental correlations, a useful methodology for estimation of droplet size distribution, which is necessary for implementing the DPM approach, was developed. Compared with the original study of Hansen et al. (1993), the developed model did provide high-quality details of fluid-flow profiles, leading to a very realistic overall picture of phase separation in all zones of the separator. The CFD simulations demonstrated that major separation inefficiencies may be encountered with the projected increase in the flow rate of produced water, which compared well with the oilfield separator experience. The CFD simulations showed that droplet breakage was common with an average rate of 76%, when dispersed droplets came into contact with the deflector baffle. Because of droplet breakup, the volume median diameter of droplets decreased to approximately 67% of the initial value. However, the droplet size distribution remained almost the same while the droplets were traveling through the gravity separation zone of the separator. Moreover, free coalescence of droplets was not a common phenomenon; hence, any positive effect of free coalescence on the separation efficiency was negligible.

Nomenclature

A_f = open area of a perforated plate, L^2, m^2
A_p = total area of a perforated plate, L^2, m^2
C = discharge coefficient for a perforated plate
C_2 = inertial resistance factor, L^{-1}, m^{-1}
$\bar{d}$ = volume mean diameter in Rosin-Rammler equation, L, μm [m]
d_{max} = maximum droplet diameter, L, μm [m]
d_{min} = minimum droplet diameter, L, μm
D = inside diameter of pipe, L, m
I = turbulence intensity
n = spread parameter in Rosin-Rammler equation

Re = Reynolds number
V = fluid velocity, L/t, m/s
V_c = superficial velocity of continuous phase, L/t, m/s
Y_d = the mass fraction of droplets with diameter greater than d
α = permeability factor, L^2, m^2
δ = thickness of a perforated plate, L, m
ΔP = pressure gradient, m/Lt^2, Pa
Δx = gradient along thickness of a perforated plate, L, m
μ = fluid viscosity, m/Lt, Pa·s
μ_c = continuous-phase viscosity, m/Lt, Pa·s
μ_d = dispersed-phase viscosity, m/Lt, Pa·s
ρ = fluid density, m/L^3, kg/m^3
ρ_c = continuous-phase density, m/L^3, kg/m^3
ρ_d = dispersed-phase density, m/L^3, kg/m^3
σ = surface tension, m/t^2, N/m

Subscripts

c = continuous
d = dispersed, a diameter
max = maximum
min = minimum
r = reduced

References

Anderson, J.D. Jr. 1995. *Computational Fluid Dynamics: The Basics with Applications*. New York: McGraw-Hill Science/Engineering/Math.

Angeli, P. and Hewitt, G.F. 2000. Drop size distributions in horizontal oil-water dispersed flows. *Chem. Eng. Sci.* **55** (16): 3133–3143. http://dx.doi.org/10.1016/s0009-2509(99)00585-0.

ANSYS. 2006a. Fluent, version 6.3.26 (commercial computational fluid dynamics simulator). Canonsburg, Pennsylvania: ANSYS Inc.

ANSYS. 2006b. Gambit, version 2.4.6 (primary pre-processor for Fluent). Canonsburg, Pennsylvania: ANSYS Inc.

Antonoff, G.N. 1907. Surface Tension at the Boundary of Two Layers. *J. Chim. Phys. Phys.-Chim. Biol.* **5**: 372–385.

AspenTech. 2003. Aspen HYSYS V3.2 Chemical Process Simulator. Burlington, Massachusetts: Aspen Technology, Inc.

Coker, A.K. 2007. *Ludwig's Applied Process Design for Chemical and Petrochemical Plants*, fourth edition. Burlington, Massachusetts: Gulf Professional Publishing.

Fluent 6.3.26 User Guide. 2006. Lebanon, New Hampshire: Fluent, Inc.

Frankiewicz, T. and Lee, C.-M. 2002. Using Computational Fluid Dynamics (CFD) Simulation to Model Fluid Motion in Process Vessels on Fixed and Floating Platforms. Paper SPE 77494 presented at the SPE Annual Technical Conference and Exhibition, San Antonio, Texas, USA, 29 Septemper–2 October. http://dx.doi.org/10.2118/77494-MS.

Frankiewicz, T., Browne, M.M., and Lee, C.-M. 2001. Reducing Separation Train Sizes and Increasing Capacity by Application of Emerging Technologies. Paper OTC 13215 presented at the Offshore Technology Conference, Houston, 30 April–3 May. http://dx.doi.org/10.4043/13215-MS.

Gosman, A.D. 1998. Developments in Industrial Computational Fluid Dynamics. *Chem. Eng. Res. Des.* **76** (2): 153–161. http://dx.doi.org/10.1205/026387698524721.

Green, D.W. and Perry, R.H. 2007. *Perry's Chemical Engineers' Handbook*, eighth edition. New York: McGraw-Hill.

Hallanger, A., Soenstaboe, F., and Knutsen, T. 1996. A Simulation Model for Three-Phase Gravity Separators. Paper SPE 36644 presented at the SPE Annual Technical Conference and Exhibition, Denver, 6–9 October. http://dx.doi.org/10.2118/36644-MS.

Hansen, E.W.M., Heitmann, H., Lakså, B. et al. 1991. Fluid Flow Modeling of Gravity Separators. *Proc.,* 5th International Conference on Multiphase Production, Cannes, France, 19-21 June, 364–380.

Hansen, E.W.M., Heitmann, H., Laska, B. et al. 1993. Numerical Simulation of Fluid Flow Behavior Inside, and Redesign of a Field Separator. *Proc.,* 6th International Conference on Multiphase Production, Cannes, France, 19–21 June, 117–129.

Heidemann, R.A., Jeje, A.A., and Mohtadi, F. 1987. *An Introduction to the Properties of Fluids and Solids*. Calgary, Alberta: The University of Calgary Press.

Helsør, T. and Svendsen, H. 2007. Experimental Characterization of Pressure Drop in Dry Demisters at Low and Elevated Pressures. *Chem. Eng. Res. Des.* **85** (3): 377–385. http://dx.doi.org/10.1205/cherd06048.

Hesketh, R.P., Fraser Russell, T.W., and Etchells, A.W. 1987. Bubble size in horizontal pipelines. *AIChE J.* **33** (4): 663–667. http://dx.doi.org/10.1002/aic.690330414.

Hinze, J.O. 1955. Fundamentals of the hydrodynamic mechanism of splitting in dispersion processes. *AIChE J.* **1** (3): 289–295. http://dx.doi.org/10.1002/aic.690010303.

Issa, R.I. 1986. Solution of the implicitly discretised fluid flow equations by operator-splitting. *J. Comput. Phys.* **62** (1): 40–65. http://dx.doi.org/10.1016/0021-9991(86)90099-9.

Karabelas, A.J. 1978. Droplet size spectra generated in turbulent pipe flow of dilute liquid/liquid dispersions. *AIChE J.* **24** (2): 170–180. http://dx.doi.org/10.1002/aic.690240203.

Kim, H. and Burgess, D.J. 2001. Prediction of Interfacial Tension between Oil Mixtures and Water. *J. Colloid Interface Sci.* **241** (2): 509–513. http://dx.doi.org/10.1006/jcis.2001.7655.

Kolmogorov, A.N. 1949. On the Breaking of Drops in Turbulent Flow. *Dokl. Akad. Nauk SSSR* **66**: 825–828.

Kolodzie, P.A. and Van Winkle, M. 1957. Discharge coefficients through perforated plates. *AIChE J.* **3** (3): 305–312. http://dx.doi.org/10.1002/aic.690030304.

Launder, B.E. and Spalding, D.B. 1972. *Mathematical Models of Turbulence*. New York: Academic Press.

Lee, C.-M., van Dijk, E., Legg, M. et al. 2004. Field Confirmation of CFD Design for FPSO-mounted Separator. Paper OTC 16137 presented at the Offshore Technology Conference, Houston, 3–6 May. http://dx.doi.org/10.4043/16137-MS.

Lee, J.M., Khan, R.I., and Phelps, D.W. 2009. Debottlenecking and Computational-Fluid-Dynamics Studies of High- and Low-Pressure Production Separators. *SPE Proj Fac & Const* **4** (4): 124–131. SPE-115735-PA. http://dx.doi.org/10.2118/115735-PA.

Levich, V.G. 1962. *Physiochemical Hydrodynamics*. Englewood Cliffs: Prentice-Hall.

Lu, Y., Lee, J.M., Phelps, D. et al. 2007. Effect of Internal Baffles on Volumetric Utilization of an FWKO--A CFD Evaluation. Paper SPE 109944 presented at the SPE Annual Technical Conference and Exhibition, Anaheim, California, USA, 11–14 November. http://dx.doi.org/10.2118/109944-MS.

Lyons, W.C. and Plisga, G.J. 2005. *Standard Handbook of Petroleum and Natural Gas Engineering*, second edition. Burlington, Massachusetts: Gulf Professional Publishing.

Poling, B.E., Prausnitz, J.M., and O'Connell, J.P. 2001. *The Properties of Gases and Liquids*, fifth edition. New York: McGraw-Hill Professional.

Pourahmadi Laleh, A. 2010. *CFD Simulation of Multiphase Separators*. PhD dissertation, University of Calgary, Calgary, Alberta, Canada (September 2010).

Rosin, P. and Rammler, E. 1933. The Laws Governing the Fitness of Powdered Coal. *J Inst Fuel* **7**: 29–36.

Sharratt, P.N. 1990. Computational Fluid Dynamics and its Application in the Process Industries. *Chemical Engineering Research Design* **68** (1): 13–18.

Shelley, S. 2007. Computational Fluid Dynamics—Power to the People. *Chem. Eng. Prog.* **103** (4): 10–13.

Streeter, V.L. and Wylie, E.B. 1985. *Fluid Mechanics*, eighth edition. New York: McGraw-Hill.

Swartzendruber, J., Fadda, D., and Taylor, D. 2005. Accommodating Last Minute Changes: Two Phase Separation Performance Validated by CFD. *Proc.,* ASME Fluids Engineering Division Summer Meeting and Exhibition, Houston, 19-23 June, 713–715.

Walas, S.M. 1990. *Chemical Process Equipment Selection and Design*. Newton, Massachusetts: Butterworth-Heinemann Series in Chemical Engineering, Butterworth-Heinemann.

Ali Pourahmadi Laleh is a research engineer with the Reservoir Simulation Group in Calgary. He has more than 11 years of experience as a research engineer, involved in rectifying industrial scale process inefficiencies and optimizing chemical plants. Pourahmadi Laleh has done research in separation technologies, coal liquefaction, and hot fluid-injection processes. He has proposed a novel approach for automatic design of the optimum distillation column sequence using genetic algorithms. He has also developed an efficient strategy for realistic simulation of oilfield separators and has provided improved design criteria for these multiphase separators. Pourahmadi Laleh holds a BS degree from Sahand University of Technology, an MSc degree from Sharif University of Technology, and a PhD degree from the University of Calgary, all in chemical engineering.

William Y. Svrcek is a professor emeritus at the University of Calgary and president of Virtual Materials Group Inc. in Calgary. Prior to joining the University of Calgary, he worked for Monsanto Company as a senior systems engineer and as an associate professor (1970–75) at the University of Western Ontario. Svrcek was also a senior partner in Hyprotech, now part of Aspen Technology, from its incorporation in 1976. As a principal, director, and president (1981–1993), he was instrumental in establishing Hyprotech as a leading international process simulation software company. Svrcek's teaching and research interests center on process-simulation control and design. He has been involved for many years in teaching a continuing education course, Computer-Aided Process Design: Oil and Gas Processing, that has been presented worldwide. He has authored or coauthored over 200 technical articles/reports and has supervised more than 50 graduate students. Svrcek holds BS and PhD degrees in chemical engineering from the University of Alberta.

Wayne D. Monnery is president of Chem-Pet Process Tech Limited in Calgary and an adjunct associate professor at the University of Calgary. He has 24 years of industrial experience as a process engineer, with recognized expertise in applied thermodynamics, process simulation, and physical properties of petroleum systems, as well as in sweet gas processing, sour gas treating, and sulfur recovery. Monnery has also worked on heavy oil and steam assisted gravity drainage (SAGD) facility simulation and design. He has done research in sulfur plant kinetics, alternative sour gas treating, water content of high-pressure acid gases for acid gas injection, and phase separation. Monnery holds a PhD degree in chemical engineering from the University of Calgary.